Three-dimensional Structures of Cyclin-Dependent Kinases and Their Inhibitor Complexes.

Ursula Schulze-Gahmen and Sung-Hou Kim

CONTENTS

1.1 INTRODUCTION

Cyclin-dependent kinases (CDKs) are eukaryotic serine/threonine protein kinases that are closely related to the prototypical Cdc2 protein (Forsburg and Nurse, 1991) and are known to associate

with cyclin-related regulatory subunits. In yeast, a single CDK (Cdc28 in the budding yeast *Saccharomyces cerevisiae* and Cdc2 in the fission yeast *Schizosaccharomyces pombe*) regulates all cell cycle transitions by forming complexes with various cyclin proteins (Forsburg and Nurse, 1991). In higher eukaryotes, at least 10 CDKs have been identified. However, only a few of them, CDC2 (CDK1) and CDK2, are involved in central cell cycle functions. Other functions include coupling of the cell cycle to extracellular signals (CDK4 and CDK6), phosphorylation of other CDKs (CAK, CDK7) and transcription (CDK7, CDK8, CDK9), and neural differentiation (CDK5) (Morgan, 1997; Sausville, 2002).

Extensive biochemical and structural studies of several of the CDKs have established a clear picture of the activation and regulatory mechanisms that determine the kinase activity in correlation with the cell cycle phases. Since the emphasis of this review is on the structural aspects of CDKs and their inhibitor complexes, we will only summarize the common activation and inhibition mechanisms of CDKs to provide a biological background for discussion and comparison of the different activation states of CDKs. These regulatory mechanisms have been previously summarized in some excellent reviews by (Jeffrey et al., 2000; Mapelli and Musacchio, 2003; Morgan, 1997; Pavletich, 1999).

1.2 OVERVIEW AND COMPARISON OF CDK STRUCTURES

Four major mechanisms appear to govern the enzymatic activity of CDKs. It seems, however, that not every mechanism is used by all CDKs. All CDK apoenzymes are inactive and require complex formation with cyclins or cyclin-like regulatory subunits as a first step of activation. The CDK5 complexes with p25 and p35 and CDK6-Vcyclin complex appear to become fully activated by this one-step mechanism (Schulze-Gahmen and Kim, 2002; Tarricone et al., 2001).

However, complete activation of other CDKs involved in cell cycle control requires phosphorylation of a conserved threonine in the activation loop (Connell-Crowley et al., 1993; Desai et al., 1992; Solomon et al., 1992). The fully active complexes can be turned off by two mechanisms: CDK inhibitory proteins can bind and inactivate the CDK-cyclin complexes (Brotherton et al., 1998; Russo et al., 1996a; Russo et al., 1998), or regulatory kinases can phosphorylate CDKs on residues in the glycine-rich loop near the N-terminus (McGowan and Russell, 1993; Norbury et al., 1991; Parker et al., 1992). A quite large number of crystal structures of different CDKs in different activation states has been solved over the last 12 years. They revealed an enormous flexibility of the CDK structures and provided a structural basis for the observed activation and inhibition mechanisms. This wealth of structural information is also extremely valuable when designing small molecule inhibitors of CDKs for the development of anti-tumor drugs. For example, if the inhibitors should be CDK specific or specifically directed against the inactive or activated form of CDKs, the available structural information can define a precise target for inhibitor design. We compare here the structures of different CDK apoenzymes, activated CDK complexes, and CDK-inhibitor complexes to highlight CDK-specific features and structural changes that are correlated with CDK activation and inhibition. Where specific CDK residues are mentioned in the discussion, residue numbering will be based on the CDK2 sequence (Fig. 1) unless specifically indicated otherwise.

1.2.1 Apoenzymes

The crystal structures of two apoenzymes, CDK2 and CDK7, have been determined to 1.8 Å and 3.0 Å, respectively (De Bondt et al., 1993; Lolli et al., 2004; Schulze-Gahmen et al., 1996). The kinases provide adjacent binding sites for ATP and protein substrate, that orient the reaction partners in such a way that the γ–phosphate of ATP faces the hydroxylated side chain on the

protein surface. Catalytic residues then promote the transfer of the phosphate group to the oxygen of the hydroxyl. CDK2 and CDK7 have 44% sequence identity and show the typical protein kinase fold. A smaller N-terminal domain is composed of a beta sheet and the large αC-helix (Taylor et al., 1992). It is connected by a linker to the larger, mostly helical C-terminal domain. ATP is bound in the cleft between the two domains so that the hydrophobic purine ring binds in a pocket close to the linker region and the phosphates are oriented outward toward the mouth of the cleft.

The CDK apoenzymes are incapable of catalyzing the phosphotransfer reaction. Their activity is blocked in two ways. First, the activation loop (residues D145 to E172 in CDK2) is folded upward from the C-terminal domain and blocks protein substrate binding. Although the activation loop is flexible in the apoenzymes and adopts somewhat different conformations in CDK2 and CDK7, it prevents peptide binding in both cases (Fig. 2). Second, essential catalytic residues are located in the catalytic loop (residues 126-132 in CDK2) (Fig. 2), in β3, and in the αC-helix. The conformation of the activation loop in inactive CDK2 and CDK7 forces a rotation of the αC-helix which leads to the incorrect positioning of several key catalytic residues and the incorrect alignment of β and γ–phosphates in ATP for an efficient in-line phosphotransfer reaction. The structures of CDK2 and CDK7 are similar with an rms deviation in Cα positions of 0.9 Å for 134 residues in the C-terminal domain and 1.2 Å for 66 residues in the N-terminal domain. The major differences between CDK2 and CDK7 occur in three regions: (1) the activation loop; (2) a region where three protein segments pack together comprising αD and the following loop (residues 92-98), the β7/β8 loop (residues 136-139), and the C-terminal region (residues 287-298); and (3) the region of the L14 loop (residues 236-240) which is part of the kinase associated phosphatase (KAP) recognition site (Song et al., 2001) and Cks1 regulatory

protein binding site in CDK2 (Bourne et al., 1996). The structural differences in region 2 and 3 may cause differences in specific interactions of CDKs with substrates or regulatory proteins. For example, members of the MAP kinase family interact with docking site sequences in their protein substrates that are spatially separate from the substrate phosphorylation sites. The structure of p38 in complex with docking peptides from two such interacting proteins show these peptides interacting at a site that is equivalent to the C-terminal region, β7/β8 loop, and αD/αE loop in CDKs (Chang et al., 2002). A similar mechanism might exist for substrate binding to CDK7, or another protein might interact with CDK7 in this region. Structural and sequence differences in region 3 were shown to be important for the regulation of kinase-associated phosphatase (KAP) activity, which is active on CDK2 but not on CDK7 (Lolli et al., 2004; Song et al., 2001).

1.2.1 Activated CDK-Cyclin Complexes

Cyclin binding to CDKs activates CDKs partially or completely, depending on the CDK. The CDK2-CyclinA complex requires an additional phosphorylation on Thr 160 for complete activation. This activation is correlated with characteristic structural changes that have been observed in the crystal structures of three activated CDKs, CDK2-Cyclin A (Jeffrey et al., 1995; Russo et al., 1996b), CDK5-p25 (Tarricone et al., 2001), and CDK6-Vcyclin (Schulze-Gahmen and Kim, 2002). The activation loop that was obstructing the binding cleft in the apoenzyme, is moved towards the C-terminal domain where it forms a binding area for the substrate protein (Fig. 3). Phosphorylation of the Thr 160 in CDK2 leads to further conformational changes in the substrate binding site causing an unusual left-handed conformation ($\Phi = 72.5^{o}$, $\Psi = 130.8^{o}$) for residue V164. The valine conformation results in the carbonyl oxygen atom being directed away

from the substrate, which has the effect that binding of any other residue except proline at the P+1 site would be unfavorable because of an uncompensated hydrogen bond from the substrate's main-chain nitrogen (Brotherton et al., 1998). The phosphorylation induced change in the substrate binding pocket in CDK2 is induced in CDK5-p25 and CDK6-Vcyclin by cyclin binding alone.

Simultaneously with the movement of the activation loop, the αC-helix is moved into the binding cleft and rotated so that the side chain of E51 in the αC-helix becomes rotated into the ATP binding pocket, where it forms ionic interactions with K33. The role of K33 is to bind to the α and β-phosphates of ATP and align them to enable the transfer of the γ-phosphate to substrate proteins (Taylor et al., 1992).

P25 and Vyclin induce very similar structural changes in CDK5 and CDK6, respectively, leading to activation of these kinases without requiring additional phosphorylation of the threonine in the activation loop. Fig. 4 shows the superposition of activated CDK5 and CDK6 on the C-terminal domain of activated CDK2. The structural elements of the C-terminal domain and the αC-helix overlap very well. Structural differences are found in the relative orientation of the N-terminal β-sheet, the tip of the activation loop, the L14-loop, and the αD/αE loop. These structural differences may indicate higher flexibility in these regions or may be the reason for differential interactions with other CDK-interacting proteins, such as KAP or protein substrates. The critical structural changes for enzymatic activation of CDKs are, however, the same for all three structures.

1.2.2 CDK-Protein Inhibitor Complexes

The active CDKs can be counteracted by two families of cell cycle inhibitory proteins. Members

of the Cip family, which include $p27^{Kip1}$, $p21^{Cip1,WAF-1}$, and $p57^{Kip2}$ bind and inhibit the active CDK-cyclin complexes (Sherr and Roberts, 1995). Members of the INK4 family, which include p15, p16, p18, and p19, are specific for CDK4 and CDK6, and can bind to either the isolated CDK subunit or its complex with cyclin D (Serrano, 1997). The INK4 inhibitors are specific for the G1 phase CDKs, whereas the Cip inhibitors have a broader CDK preference. Crystal structures of a 69-amino-acid peptide from $p27^{Kip1}$ bound to CDK2-CyclinA (Russo et al., 1996a) and $p16^{INK4}$ and $p19^{INK4}$ in complex with CDK6 (Brotherton et al., 1998; Russo et al., 1998) revealed that both types of inhibitors induce large changes in the shape of the ATP and substrate binding site of CDKs. The p27-peptide binds with its N-terminal part to cyclinA, and with its C-terminal part to the N-terminal domain of CDK2. The conserved 'LFG' motif in p27 is inserted in a pocket on the face of cyclinA without changing the conformation of cyclin A (Fig. 5A). The same 'LFG' sequence motif is found in tight binding substrates of CDK2-CyclinA (Zhu et al., 1995). The p27-peptide then stretches over to the N-terminal domain of CDK2, where its binding induces large structural changes in the kinase. First, the β-turn segment of p27 flattens the β-sheet of the kinase. Second, the β-strand segment of p27 replaces the first β-strand of the CDK2 sheet, which becomes disordered. Third, the carboxy-terminal segment of the p27-peptide, the 3_{10}-helix, binds deep within the active site-cleft and prevents ATP binding by mimicking the ATP substrate in its position and the contacts it makes to active site groups (Fig. 5A).

The $p16^{INK4}$ and $p19^{INK4}$ inhibitors also take advantage of the kinase flexibility to distort the catalytic cleft and prevent the necessary activating structural changes. p16 and p19 consist of four and five ankyrin repeats, respectively. Each ankyrin repeat has a structure that resembles the letter L (Gorina and Pavletich, 1996), with a pair of antiparallel helices forming the stem and

a β-hairpin forming the base. The L-shaped repeats stack to give an extended concave surface (Fig. 5B). CDK6-bound p16 and p19 have very similar structures (Brotherton et al., 1998; Russo et al., 1998) with p19 having an extra repeat added at the part of the structure furthest away from CDK6. p19 binds to one side of the catalytic cleft opposite to the cyclin binding site. The concave site of the p19 molecule binds to the β-sheet in the N-terminal domain of CDK6, and the ends of the helices of ankyrin repeats 1 to 3 bind to the C-terminal domain where they interact with the activation loop and with structural elements of the catalytic cleft. Like the inactive CDK2 apoenzyme, p19-bound CDK6 does not have any of the activating changes. However, p19 binding induces structural distortions in CDK6 that move it further away from the active structure. The N-terminal and C-terminal domains are twisted away from each other, distorting the cyclin binding site and preventing the translocation of the αC-helix into the binding cleft. The ATP binding site is distorted because of p19 contacts with CDK6 residues in the linker region between the N-terminal and C-terminal domain and in the catalytic cleft, and because of the relative domain movements. The p19-CDK6 structures indicate that the inhibitor-kinase interactions result in extensive movements of the N-terminal domain of the kinase relative to the C-terminal domain, inhibiting productive binding with ATP and movement of the αC-helix to its active conformation. The distortions of the cyclin binding site are consistent with the observation that p16 binding weakens the affinity of cyclinD for CDK4 and CDK6 (Parry et al., 1995; Ragione et al., 1996).

1.2.4 The ATP Binding Pocket in Active and Inactive CDKs

All of the known chemical inhibitors of CDKs are binding in the ATP binding pocket located between the two kinase domains. Hence, a detailed structural characterization of the ATP

binding pocket is very valuable for rational drug design efforts. Since residues lining the ATP binding pocket in different CDKs are quite conserved, we will describe here the ATP binding pocket in the high resolution structures of activated CDK2 (Brown et al., 1999b) and the CDK2 apoenzyme (De Bondt et al., 1993; Schulze-Gahmen et al., 1996) (Figs. 6, 7). In the ternary complex of CDK2 with ATP and a substrate peptide, the purine ring of ATP is binding close to the hinge region connecting the N-terminal and C-terminal domain (residues 81-84). The N1 and N6 nitrogen of the adenine base form hydrogen bonds with the peptide bond nitrogen of L83 and oxygen of E81, respectively. Hydrogen bonds with the same hinge residue atoms are conserved for most molecules binding in the kinase active site, but they can be formed from a diverse range of heterocyclic frameworks. In fact, satisfying the hydrogen bond-donating capacity of the backbone nitrogen of L83 is the only conserved feature of all CDK2/inhibitor complex structures determined to date (Davies et al., 2002b). The adenine ring is also sandwiched between a number of hydrophobic residues, including I10, A31, F82, and L134. The back wall of the ATP binding cleft is formed by the side chain of F80, the "gatekeeper" residue (Liu et al., 1999; Schindler et al., 1999). Although the adenine ring of ATP does not come close to the Phe80 side chain, other bound inhibitors pack hydrophobic groups into this site and take advantage of hydrophobic interactions with the phenyl ring. Members of other kinase families have a much larger hydrophobic pocket in this area, due to a smaller "gatekeeper" residue. The difference in size of the hydrophobic pocket has been successfully used to create kinase specific inhibitors (Cohen et al., 2005; Liu et al., 1999; Schindler et al., 1999; Tong et al., 1997). The ribose and phosphate moiety of ATP binds in an open cleft formed in part by the flexible glycine loop (residues 11-18), residues from the catalytic loop (residues 126-132), K33, and D145 (Fig. 7). The ribose and phosphate atoms form a network of hydrogen bonds with side-chain and main-chain atoms

lining the cleft, as well as with water molecules in the binding pocket. A single Mg ion is coordinated to oxygens from ATP α and γ-phosphates, N132, and D145 (Fig. 6). The ATP binding pockets of the activated CDK2 enzyme and inactive CDK2 apoenzyme are structurally similar. After superposition of the molecules on the C-terminal domain, relatively small shifts are observed in the position of residues in the N-terminal domain adjacent to the adenine ring. These shifts originate from the rotation of the N-terminal domain relative to the C-terminal domain after activation of the CDK2 apoenzyme. Much larger shifts are observed for residues 11-18 in the glycine loop, which contact the ribose and phosphates of the bound ATP. Larger structural difference are also seen in the position of K33 and E51. E51 is located in the αC-helix which is rotated and moved into the binding pocket after cyclin binding to CDK2 (Jeffrey et al., 1995). Before CDK2 activation E51 points away from the ATP binding pocket, but moves into the vicinity of the pocket to form an ionic interactions with K33 after CDK2 activation. K33 is directly interacting with the ATP phosphates and also with some inhibitor molecules (Davies et al., 2001; Lu et al., 2005; Meijer et al., 2000). E51 does not interact with ATP directly, but it was shown to interact with a bound inhibitor to CDK6 (Lu et al., 2005). Structural differences in the ATP binding pocket between inactive and activated CDKs may need to be taken into account for drug design studies, especially if the inhibitor molecule extends beyond the adenine binding region of the ATP binding pocket (Davies et al., 2001). Inhibitor interactions with residues that show structural differences between the two kinase states, such as K33 and E51, can be used to design inhibitors with preference for the active kinase.

1.3. Comparison of Inhibitor Complex Structures

The central role that CDKs play in cell cycle control and the high incidence of genetic alterations

of CDKs or their regulators in a number of cancers make CDKs an important target for therapeutic intervention in various proliferative diseases including cancer (Sielecki et al., 2000). Hence, considerable efforts were made to screen for and design CDK-specific inhibitors. To date, a large number of chemically diverse inhibitors with high affinities for CDK1, CDK2, and CDK5 are available and several of them have entered clinical trials to treat cancer (Blagden and de Bono, 2005; Meijer et al., 1999; Senderowicz and Sausville, 2000). Drug design of CDK2-specific inhibitors was greatly helped by the high resolution X-ray structures of CDK2 and its inhibitor complexes. In the following sections, we will highlight the structural features of several CDK-inhibitor complexes and suggest a structural basis for the lower binding affinities of some of these inhibitors for CDK4 and CDK6.

1.3.1. Interactions of CDK2 Specific Inhibitors in the ATP Binding Site

Over the last ten years, a large number of heterocyclic CDK inhibitors with a variety of chemical scaffolds have been identified (Table 1). The compounds can be grouped into those that non-specifically inhibit all CDKs and often other protein kinases, those that are specific for the group including CDK1, CDK2, and CDK5, and those that are specific for CDK4 and CDK6. CDK4 and CDK6 form a subgroup within the CDKs based on sequence similarities. For simplicity, we will call the inhibitors of the second group CDK2-specific inhibitors because most of the structural work was performed on CDK2 complexes. The structures of the first CDK2 complexes with CDK2-specific purine based inhibitors, such as olomoucine (Schulze-Gahmen et al., 1995), roscovitine (De Azevedo et al., 1997), and purvalanol (Gray et al., 1998) showed that the aromatic ring system is bound in a different orientation than in the natural ligand ATP to make room for the larger substituent groups on the purine ring. The hydrogen bonds from the backbone

atoms of L83 and E81 in CDK2 to the adenine base in ATP are conserved (Fig. 7, 8), although with different partner atoms in the substituted purine rings of the inhibitors. Subsequently, other compounds with a variety of scaffolds were identified as more or less specific inhibitors of CDK2. The binding mode for many of these inhibitors was determined by crystallographic studies of their complexes with the CDK2-apoenzyme. Table 1 shows a list of selected CDK inhibitors whose structure was determined in complex with one of the CDKs. Comparative analysis of the binding modes of many of these inhibitors revealed some common features. 1) The hydrophobic core of the inhibitor molecule is sandwiched between the two kinase domains, forming contacts with hydrophobic residues such as I10, A31, F82, and L134. 2) High affinity inhibitors form two or three conserved hydrogen bonds with back-bone atoms in the hinge region of CDK2 (Davies et al., 2002b). 3) Many inhibitors fill out the hydrophobic pocket in front of the gate keeper residue F80 with hydrophobic groups. 4) The specificity of CDK-inhibitor interactions is most likely based on inhibitor interactions with the less conserved hinge region and specificity area (residues 84-89) which is bordering the ATP binding site from the outside of the cleft (Fig. 7). The amino acid sequence for different CDKs is less conserved in these areas (Fig. 1) and can contribute to the CDK specificity of a ligand. Examples of the structures of three inhibitor complexes with varying specificity for CDK2 are shown in Fig. 8.

1.3.2. Structural Basis for CDK Specificity

Analysis of the complex structures of CDK2 with inhibitors lead to the suggestion that the kinase specificity of many of these inhibitors is based on their interactions with residues in the specificity region that are less conserved among different CDKs. The availability of a structure the active CDK6-Vcyclin complex (Lu et al., 2005; Schulze-Gahmen and Kim, 2002) provides

the opportunity to model CDK2-specific inhibitors into the CDK6 binding pocket by superimposing the respective kinase structures, followed by optimization of the inhibitor orientation to satisfy the conserved hydrogen bonds between inhibitor and atoms in the hinge region of CDK6. Using this procedure, we placed the CDK2-specific inhibitors olomoucine (Schulze-Gahmen et al., 1995) and NU6102 (Davies et al., 2002a) into the ATP binding pocket of CDK6-Vcyclin, as well as the less specific hymenialdisine (Meijer et al., 2000) and aloisine A (Mapelli et al., 2005; Mettey et al., 2003). The placement of the olomoucine ligand results in several close contacts between the N7 atom of the adenine ring and the $H100^{CDK6}$ side chain (F82 in CDK2), and between the benzylamino group of the inhibitor and back-bone atoms of residues 102 and 103 (84 and 85 in CDK2) (Fig. 9). The unfavorable interactions with the H100 side chain cannot be easily relieved by rotating the histidine side chain because it interacts with the side chain of $F39^{CDK6}$. Both H100 and F39 are unique to CDK4 and CDK6 and are replaced by phenylalanine and a small hydrophobic residue in the other CDKs (Fig. 1).

The docking of NU6102 into the binding pocket of CDK6 leads to an even larger number of unfavorably close contacts (Fig. 9). Close interactions with the side chain of $H100^{CDK6}$, back-bone atoms of residues 102 and 103, and with the side chain of T^{107} would prevent a tight binding of NU6102 to the active CDK6-Vcyclin complex. The underlying reason for the different inhibitor interactions in CDK2 and CDK6 is a conformational difference in the hinge region. If superimposed on atoms of the C-terminal domain, the atom positions start diverging at residue 103 (85 in CDK2) and continue doing so towards the N-terminal domain. The structural differences between CDK6 and CDK2 in the hinge region are very similar in the comparison of CDK6 with the inactive CDK2, complexed with olomoucine, and with active CDK2-cyclinA,

complexed with NU6102. Hence, this difference is likely to be caused by sequence differences rather than by different crystal forms or CDK activation states which might induce different domain rotations and result in different hinge conformations. The fact that the hinge residue $H100^{CDK6}$ is unique to CDK4 and 6 and forms a close contact with the CDK4/6 conserved residue $F39^{CDK6}$ also supports the possibility that sequence differences in the hinge region might induce a different conformation in the CDK6 hinge region.

In contrast to the close contacts found in the CDK6-model complexes with CDK2 inhibitors of high specificity, we found few close interactions in the model of hymenialdisine bound to CDK6, and no significant bad contacts in the model with aloisine A. Only the Br atom in hymenialdisine is positioned too close to $Q103^{CDK6}$ in our CDK6-complex model, possibly explaining the lower IC_{50} value of hymenialdisine for CDK6 compared to CDK2 (Table1). The observations from these CDK6-inhibitor models agree quite well with the relative affinities of the CDK inhibitors for different CDKs and suggest that residues in the hinge region as well as the specificity region can contribute to the specificity of certain CDK inhibitors.

Recently, some highly specific inhibitors of CDK4 and CDK6 have been identified whose chemical structure is based on the pyrido[2,3-d]pyrimidin-7-one scaffold (Fry et al., 2004; VanderWel et al., 2005). A complex structure of these inhibitors with CDK4 or CDK6 would be extremely valuable for the understanding of the structural basis of their specificity and for the future design of CDK4/6 specific inhibitors.

Acknowledgements

Research was supported by a grant from the National Institute of Health (R29 AI4204101) to USG and ???? to SHK.

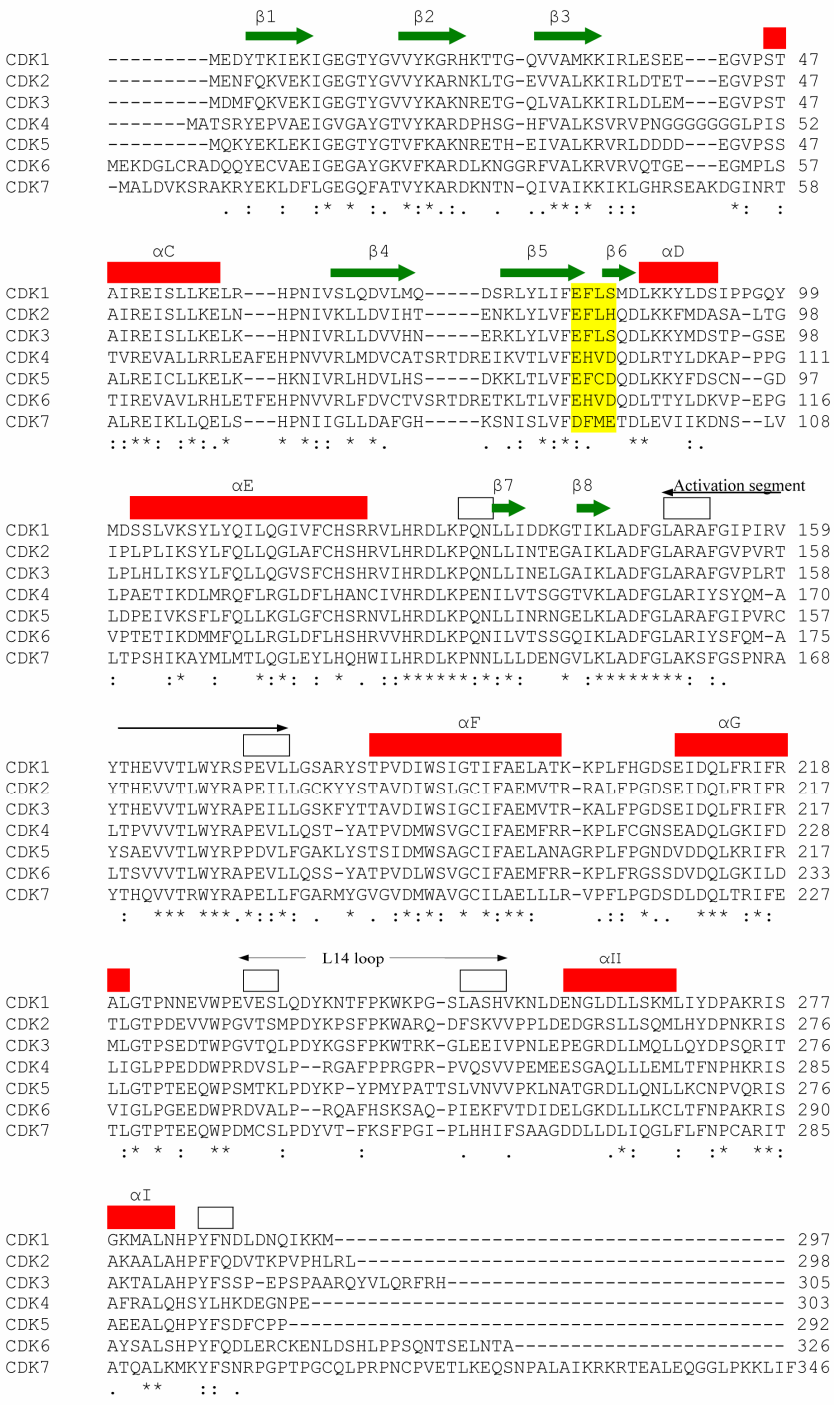

Fig. 1 Sequence alignment of human CDK1 to CDK7. The secondary structures for inactive CDK2 (De Bondt et al., 1993; Schulze-Gahmen et al., 1996) are indicated above the sequences. Residues in the hinge region between the N-terminal and C-terminal domain are highlighted with a yellow background.

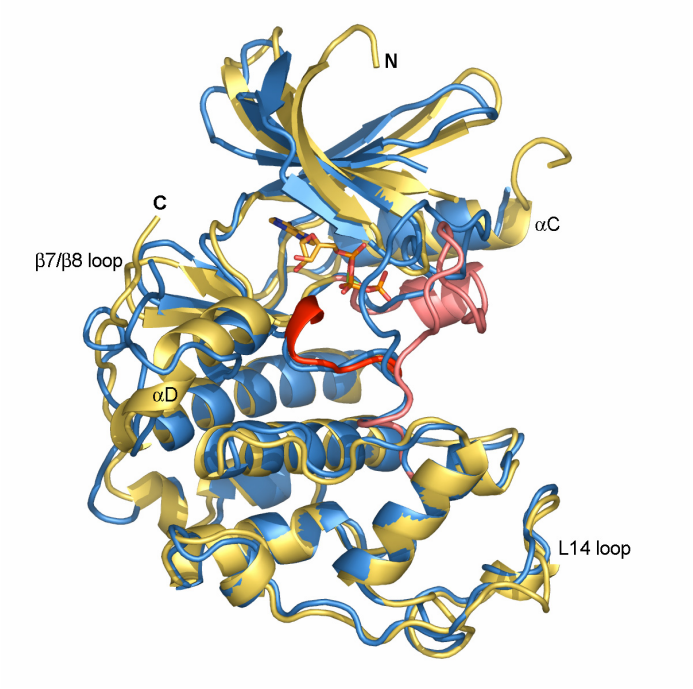

Fig. 2 CDK2 and CDK7 apoenzymes superimposed on the C-terminal domain. CDK2 is shown in yellow, CDK7 in blue. The catalytic loop and activation loop in CDK2 are drawn in red and salmon.

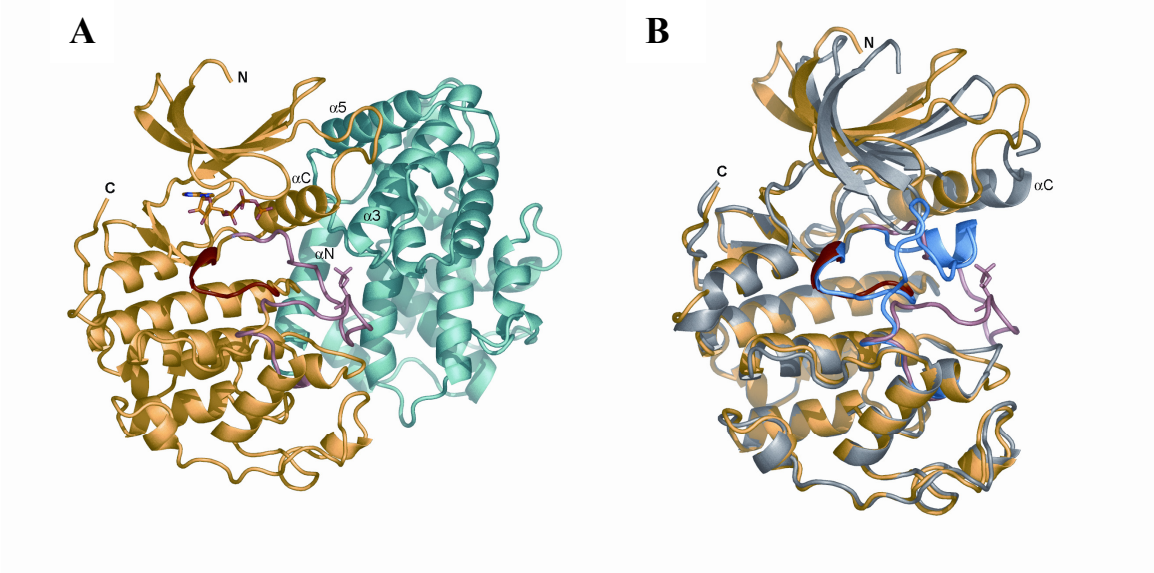

Fig. 3 (A) Phosphorylated CDK2-CyclinA. (B) CDK2 apoenzyme in gray and activated CDK2 in yellow were superimposed. The catalytic loop and activation loop in the activated CDK2 are drawn in red and salmon (blue in the apoenzyme).

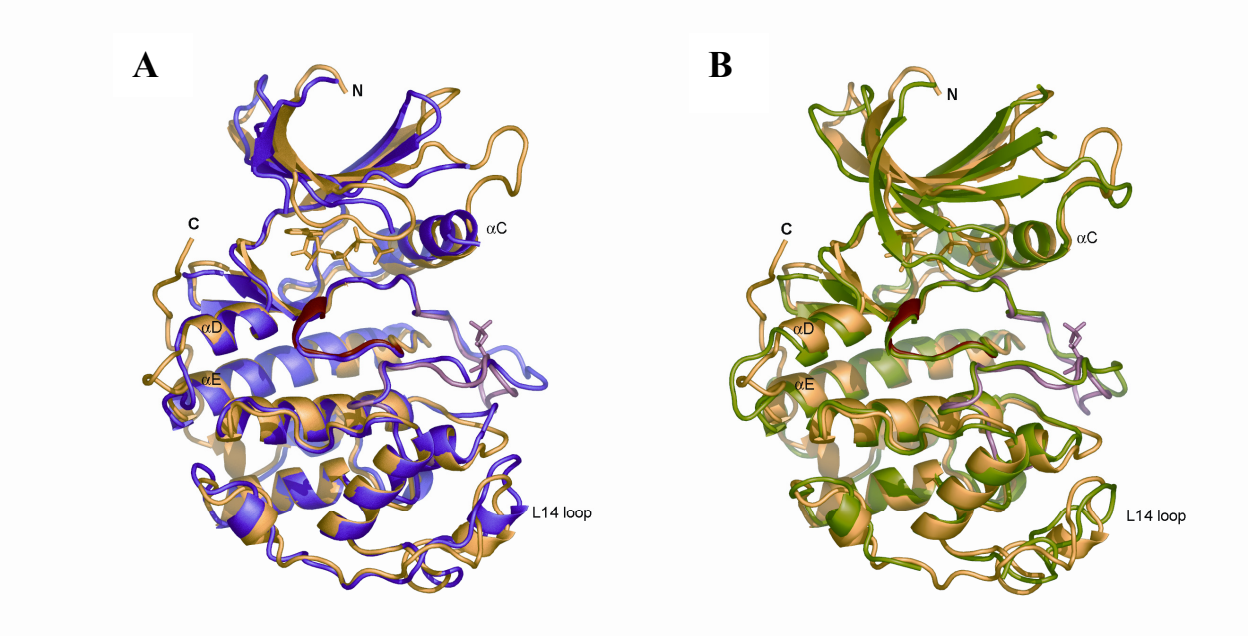

Fig. 4 Superposition of activated CDK5 and CDK6 onto activated CDK2. CDK5 from the p25 complex (A) and CDK6 from the ternary CDK6-Vcyclin-fisetin complex (B) were superimposed onto the C-terminal domain of activated CDK2-CyclinA complex. CDK2 is shown in yellow, CDK5 in purple, and CDK6 in green. The catalytic loop of CDK2 is highlighted in red, and the activation loop in salmon. Atoms of the phosphorylated threonine residue in the activation loop are shown as stick model.

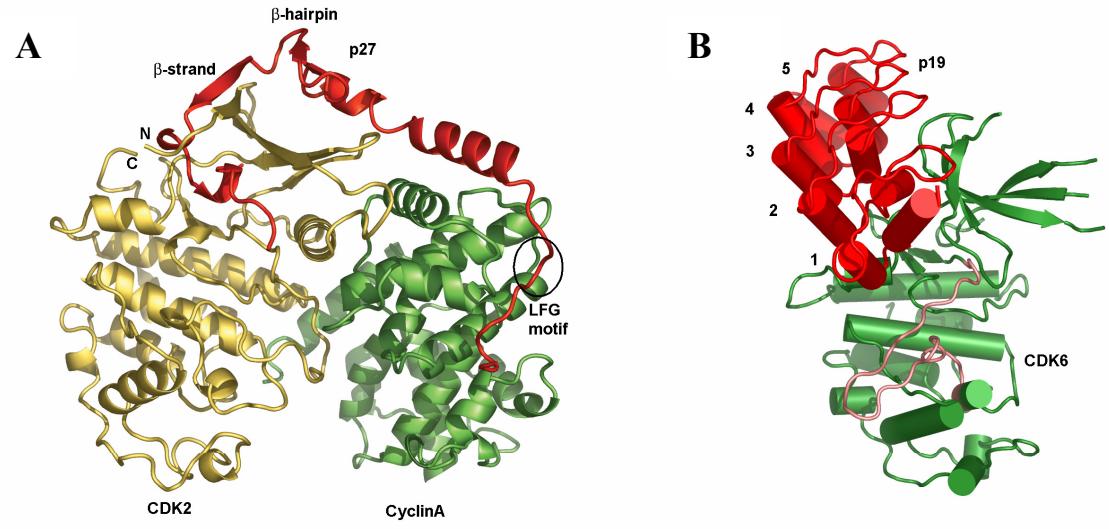

Fig. 5 Structures of CDK-Inhibitor complexes. (A) The $p27^{KIP1}$ inhibitor is bound in a ternary complex to CDK2 and cyclinA. The inhibitor is shown in red, CDK2 in yellow, and cyclinA in green. (B) The $p19^{INK4}$ inhibitor, shown in red, is bound to CDK6, shown in green.

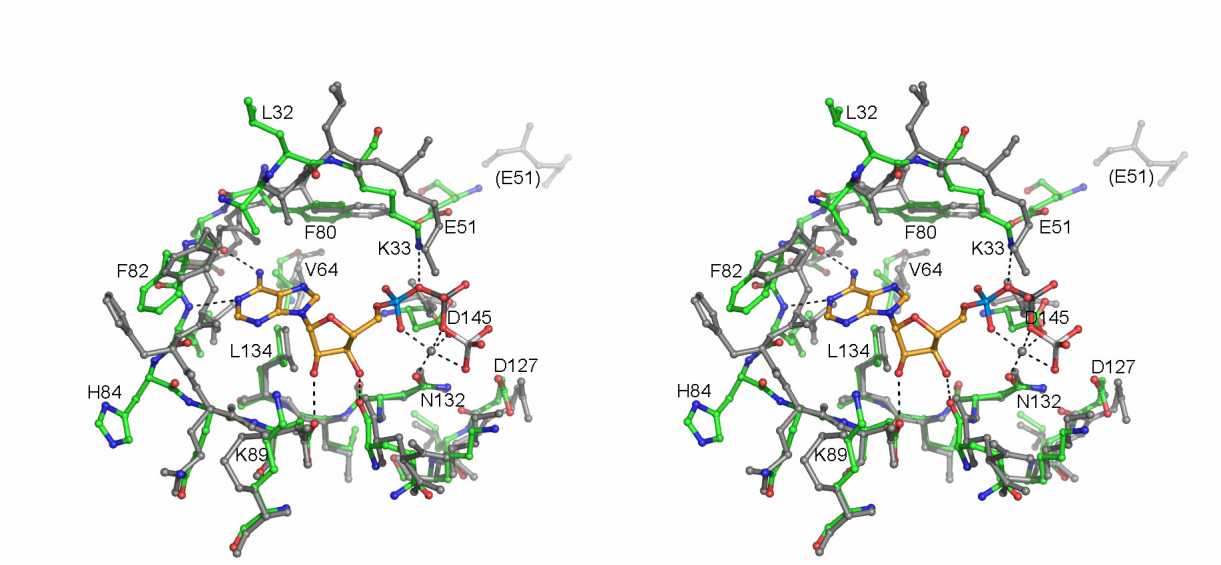

Fig. 6 Stereo drawing of the ATP binding pocket in CDK2. Residues 11-18 that form the glycine loop were omitted for clarity. The binding pocket in the activated CDK2 is shown in green with bound ATP in yellow and the Mg ion as a grey sphere. The structure of the binding pocket in the CDK2 apoenzyme is shown in grey. Hydrogen bonds are drawn as broken lines.

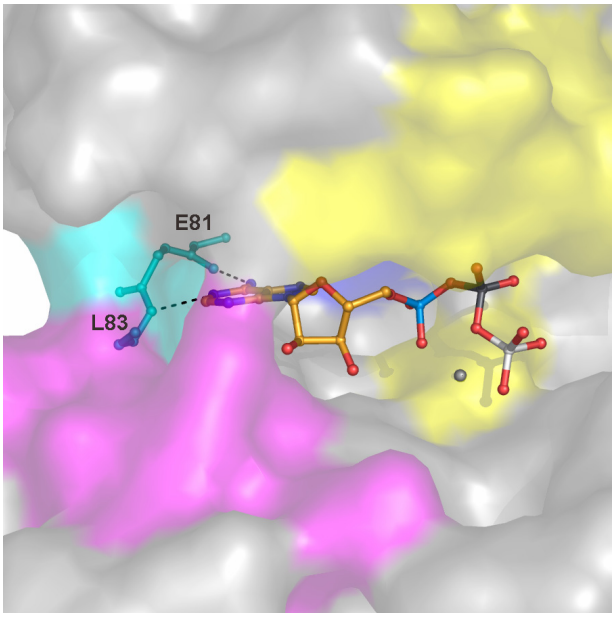

Fig. 7 Surface representation of the ATP binding pocket in CDK2 (Brown et al., 1999a). The surface is colored by pocket regions (Davies et al., 2002b). The hinge region is shown in cyan, with the back bone of residues 81 to 83 draw as stick model. Conserved hydrogen bonds with the hinge region are shown as broken lines. The F80 pocket is colored blue, the ribose and phosphate binding cleft yellow, and the specificity region purple. Bound ATP with one Mg ion is draw as a stick model.

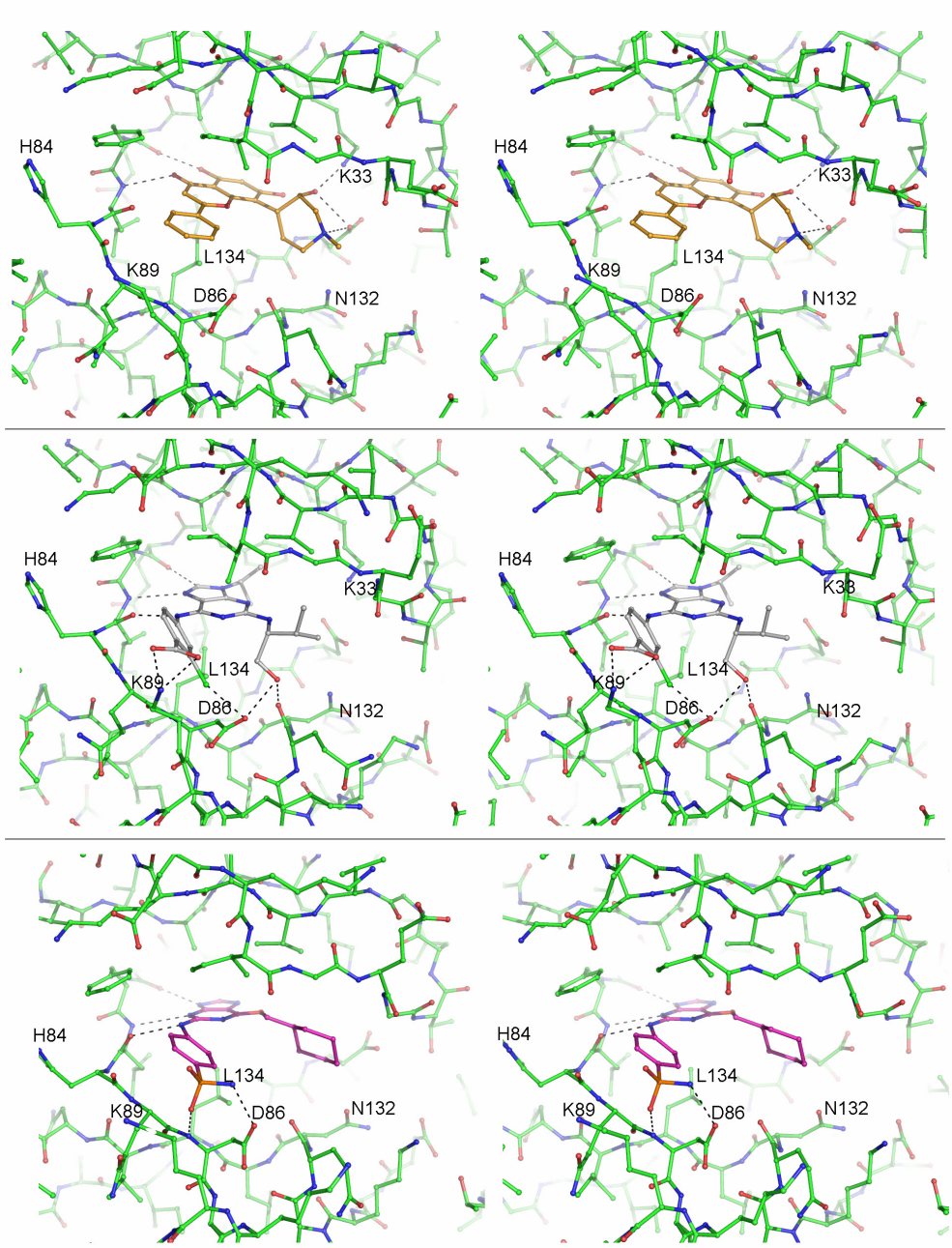

Fig. 8 Structure of the binding pocket of three CDK2-inhibitor complexes. The top shows the complex with the non-specific inhibitor des-chloro-flavopiridol. There are few contacts of the inhibitor with residues in the specificity region of the binding pocket. The middle panel shows the interactions of CDK2 with the highly specific inhibitor purvalanol B. There are many interactions with the specificity region. However, the inhibitor fills very little space in the area of the binding pocket that binds the ribose and phosphates of ATP. The bottom panel shows the interactions with NU6102, another CDK2-specific inhibitor. There are a number of interactions with the specificity region. The inhibitor also fills the ribose binding pocket with the cyclo-hexylmethyl group of the inhibitor. Hydrogen bonds between inhibitors and CDK2 are shown in black broken lines.

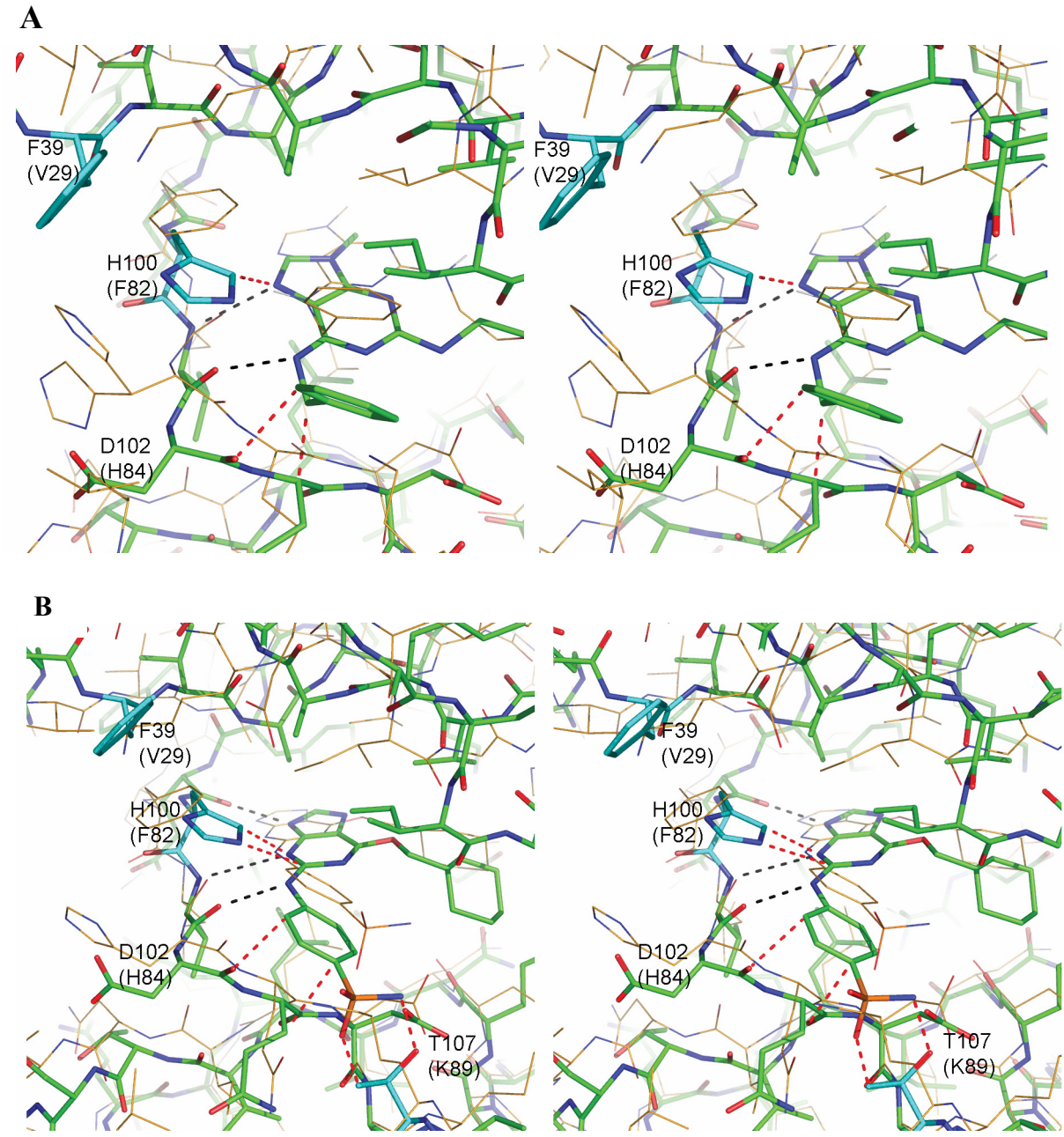

Fig. 9 Stereo drawings of the ATP binding pocket of CDK6 with CDK2 specific inhibitors olomoucine (A) and NU6102 (B) modeled into the binding pocket. The structures of the active CDK6 and the modeled inhibitor are shown as stick models in green with CDK4/6 specific sequence changes highlighted in cyan. The structure of the corresponding CDK2-inhibitor complex is drawn with thin lines in dark yellow. Conserved hydrogen bonds, used to place the inhibitor into the binding pocket, are represented by black dashed lines. Unfavorably close contacts between the inhibitor and CDK6 are shown as dashed red lines. Residue labeling refers to the CDK6 sequence with labels for CDK2 displayed in brackets.

REFERENCES

Blagden, S., and de Bono, J. (2005). Drugging cell cycle kinases in cancer therapy. Curr Drug Targets *6*, 325-335.

Bourne, Y., Watson, M. H., Hickey, M. J., Holmes, W., Rocque, W., Reed, S. I., and Tainer, J. A. (1996). Crystal structure and mutational analysis of the human CDK2 kinase complex with cell cycle-regulatory protein CksHs1. Cell *84*, 863-874.

Brotherton, D. H., Dhanaraj, V., Wick, S., Brizuela, L., Domaille, P. J., Volyanik, E., Xu, X., Parisini, E., Smith, B. O., Archer, S. J.*, et al.* (1998). Crystal structure of the complex of the cyclin D-dependent kinase Cdk6 bound to the cell-cycle inhibitor p19INK4d. Nature *395*, 244-250.

Brown, N. R., Noble, M. E., Endicott, J. A., and Johnson, L. N. (1999a). The structural basis for specificity of substrate and recruitment peptides for cyclin-dependent kinases. Nat Cell Biol *1*, 438-443.

Brown, N. R., Noble, M. E., Lawrie, A. M., Morris, M. C., Tunnah, P., Divita, G., Johnson, L. N., and Endicott, J. A. (1999b). Effects of phosphorylation of threonine 160 on cyclin-dependent kinase 2 structure and activity. J Biol Chem *274*, 8746-8756.

Chang, C. I., Xu, B. E., Akella, R., Cobb, M. H., and Goldsmith, E. J. (2002). Crystal structures of MAP kinase p38 complexed to the docking sites on its nuclear substrate MEF2A and activator MKK3b. Mol Cell *9*, 1241-1249.

Cohen, M. S., Zhang, C., Shokat, K. M., and Taunton, J. (2005). Structural bioinformatics-based design of selective, irreversible kinase inhibitors. Science *308*, 1318-1321.

Connell-Crowley, L., Solomon, M. J., Wei, N., and Harper, J. W. (1993). Phosphorylation independent activation of human cyclin-dependent kinase 2 by cyclin A in vitro. Mol Biol Cell *4*, 79-92.

Davies, T. G., Bentley, J., Arris, C. E., Boyle, F. T., Curtin, N. J., Endicott, J. A., Gibson, A. E., Golding, B. T., Griffin, R. J., Hardcastle, I. R.*, et al.* (2002a). Structure-based design of a potent purine-based cyclin-dependent kinase inhibitor. Nat Struct Biol *9*, 745-749.

Davies, T. G., Pratt, D. J., Endicott, J. A., Johnson, L. N., and Noble, M. E. (2002b). Structure-based design of cyclin-dependent kinase inhibitors. Pharmacol Ther *93*, 125-133.

Davies, T. G., Tunnah, P., Meijer, L., Marko, D., Eisenbrand, G., Endicott, J. A., and Noble, M. E. (2001). Inhibitor binding to active and inactive CDK2: the crystal structure of CDK2-cyclin A/indirubin-5-sulphonate. Structure (Camb) *9*, 389-397.

De Azevedo, W. F., Leclerc, S., Meijer, L., Havlicek, L., Strnad, M., and Kim, S. H. (1997). Inhibition of cyclin-dependent kinases by purine analogues: crystal structure of human cdk2 complexed with roscovitine. Eur J Biochem *243*, 518-526.

De Bondt, H. L., Rosenblatt, J., Jancarik, J., Jones, H. D., Morgan, D. O., and Kim, S. H. (1993). Crystal structure of cyclin-dependent kinase 2. Nature *363*, 595-602.

Desai, D., Gu, Y., and Morgan, D. O. (1992). Activation of human cyclin-dependent kinases in vitro. Mol Biol Cell *3*, 571-582.

Forsburg, S. L., and Nurse, P. (1991). Cell cycle regulation in the yeasts Saccharomyces cerevisiae and Schizosaccharomyces pombe. Annu Rev Cell Biol *7*, 227-256.

Fry, D. W., Harvey, P. J., Keller, P. R., Elliott, W. L., Meade, M., Trachet, E., Albassam, M., Zheng, X., Leopold, W. R., Pryer, N. K., and Toogood, P. L. (2004). Specific inhibition of cyclin-dependent kinase 4/6 by PD 0332991 and associated antitumor activity in human tumor xenografts. Mol Cancer Ther *3*, 1427-1438.

Gorina, S., and Pavletich, N. P. (1996). Structure of the p53 tumor suppressor bound to the ankyrin and SH3 domains of 53BP2. Science *274*, 1001-1005.

Gray, N. S., Wodicka, L., Thunnissen, A. M., Norman, T. C., Kwon, S., Espinoza, F. H., Morgan, D. O., Barnes, G., LeClerc, S., Meijer, L.*, et al.* (1998). Exploiting chemical libraries, structure, and genomics in the search for kinase inhibitors. Science *281*, 533-538.

Jeffrey, P. D., Russo, A. A., Polyak, K., Gibbs, E., Hurwitz, J., Massague, J., and Pavletich, N. P. (1995). Mechanism of CDK activation revealed by the structure of a cyclinA-CDK2 complex. Nature *376*, 313-320.

Jeffrey, P. D., Tong, L., and Pavletich, N. P. (2000). Structural basis of inhibition of CDK-cyclin complexes by INK4 inhibitors. Genes Dev *14*, 3115-3125.

Liu, Y., Bishop, A., Witucki, L., Kraybill, B., Shimizu, E., Tsien, J., Ubersax, J., Blethrow, J., Morgan, D. O., and Shokat, K. M. (1999). Structural basis for selective inhibition of Src family kinases by PP1. Chem Biol *6*, 671-678.

Lolli, G., Lowe, E. D., Brown, N. R., and Johnson, L. N. (2004). The crystal structure of human CDK7 and its protein recognition properties. Structure (Camb) *12*, 2067-2079.

Lu, H., Chang, D. J., Baratte, B., Meijer, L., and Schulze-Gahmen, U. (2005). Crystal structure of a human cyclin-dependent kinase 6 complex with a flavonol inhibitor, fisetin. J Med Chem *48*, 737-743.

Mapelli, M., Massimiliano, L., Crovace, C., Seeliger, M. A., Tsai, L. H., Meijer, L., and Musacchio, A. (2005). Mechanism of CDK5/p25 binding by CDK inhibitors. J Med Chem *48*, 671-679.

Mapelli, M., and Musacchio, A. (2003). The structural perspective on CDK5. Neurosignals *12*, 164-172.

McGowan, C. H., and Russell, P. (1993). Human Wee1 kinase inhibits cell division by phosphorylating p34cdc2 exclusively on Tyr15. Embo J *12*, 75-85.

Meijer, L., Leclerc, S., and Leost, M. (1999). Properties and potential-applications of chemical inhibitors of cyclin-dependent kinases. Pharmacol Ther *82*, 279-284.

Meijer, L., Thunnissen, A. M., White, A. W., Garnier, M., Nikolic, M., Tsai, L. H., Walter, J., Cleverley, K. E., Salinas, P. C., Wu, Y. Z.*, et al.* (2000). Inhibition of cyclin-dependent kinases, GSK-3beta and CK1 by hymenialdisine, a marine sponge constituent. Chem Biol *7*, 51-63.

Mettey, Y., Gompel, M., Thomas, V., Garnier, M., Leost, M., Ceballos-Picot, I., Noble, M., Endicott, J., Vierfond, J. M., and Meijer, L. (2003). Aloisines, a new family of CDK/GSK-3 inhibitors. SAR study, crystal structure in complex with CDK2, enzyme selectivity, and cellular effects. J Med Chem *46*, 222-236.

Morgan, D. O. (1997). Cyclin-dependent kinases: engines, clocks, and microprocessors. Annu Rev Cell Dev Biol *13*, 261-291.

Norbury, C., Blow, J., and Nurse, P. (1991). Regulatory phosphorylation of the p34cdc2 protein kinase in vertebrates. Embo J *10*, 3321-3329.

Parker, L. L., Atherton-Fessler, S., and Piwnica-Worms, H. (1992). p107wee1 is a dual-specificity kinase that phosphorylates p34cdc2 on tyrosine 15. Proc Natl Acad Sci U S A *89*, 2917-2921.

Parry, D., Bates, S., Mann, D. J., and Peters, G. (1995). Lack of cyclin D-Cdk complexes in Rb-negative cells correlates with high levels of p16INK4/MTS1 tumour suppressor gene product. Embo J *14*, 503-511.

Pavletich, N. P. (1999). Mechanisms of cyclin-dependent kinase regulation: structures of Cdks,

their cyclin activators, and Cip and INK4 inhibitors. J Mol Biol *287*, 821-828.
Ragione, F. D., Russo, G. L., Oliva, A., Mercurio, C., Mastropietro, S., Pietra, V. D., and Zappia, V. (1996). Biochemical characterization of p16INK4- and p18-containing complexes in human cell lines. J Biol Chem *271*, 15942-15949.
Russo, A. A., Jeffrey, P. D., Patten, A. K., Massague, J., and Pavletich, N. P. (1996a). Crystal structure of the p27Kip1 cyclin-dependent-kinase inhibitor bound to the cyclin A-Cdk2 complex. Nature *382*, 325-331.
Russo, A. A., Jeffrey, P. D., and Pavletich, N. P. (1996b). Structural basis of cyclin-dependent kinase activation by phosphorylation. Nat Struct Biol *3*, 696-700.
Russo, A. A., Tong, L., Lee, J. O., Jeffrey, P. D., and Pavletich, N. P. (1998). Structural basis for inhibition of the cyclin-dependent kinase Cdk6 by the tumour suppressor p16INK4a. Nature *395*, 237-243.
Sausville, E. A. (2002). Complexities in the development of cyclin-dependent kinase inhibitor drugs. Trends Mol Med *8*, S32-37.
Schindler, T., Sicheri, F., Pico, A., Gazit, A., Levitzki, A., and Kuriyan, J. (1999). Crystal structure of Hck in complex with a Src family-selective tyrosine kinase inhibitor. Mol Cell *3*, 639-648.
Schulze-Gahmen, U., Brandsen, J., Jones, H. D., Morgan, D. O., Meijer, L., Vesely, J., and Kim, S. H. (1995). Multiple modes of ligand recognition: crystal structures of cyclin-dependent protein kinase 2 in complex with ATP and two inhibitors, olomoucine and isopentenyladenine. Proteins *22*, 378-391.
Schulze-Gahmen, U., De Bondt, H. L., and Kim, S. H. (1996). High-resolution crystal structures of human cyclin-dependent kinase 2 with and without ATP: bound waters and natural ligand as guides for inhibitor design. J Med Chem *39*, 4540-4546.
Schulze-Gahmen, U., and Kim, S. H. (2002). Structural basis for CDK6 activation by a virus-encoded cyclin. Nat Struct Biol *9*, 177-181.
Senderowicz, A. M., and Sausville, E. A. (2000). Preclinical and clinical development of cyclin-dependent kinase modulators. J Natl Cancer Inst *92*, 376-387.
Serrano, M. (1997). The tumor suppressor protein p16INK4a. Exp Cell Res *237*, 7-13.
Sherr, C. J., and Roberts, J. M. (1995). Inhibitors of mammalian G1 cyclin-dependent kinases. Genes Dev *9*, 1149-1163.
Sielecki, T. M., Boylan, J. F., Benfield, P. A., and Trainor, G. L. (2000). Cyclin-dependent kinase inhibitors: useful targets in cell cycle regulation. J Med Chem *43*, 1-18.
Solomon, M. J., Lee, T., and Kirschner, M. W. (1992). Role of phosphorylation in p34cdc2 activation: identification of an activating kinase. Mol Biol Cell *3*, 13-27.
Song, H., Hanlon, N., Brown, N. R., Noble, M. E., Johnson, L. N., and Barford, D. (2001). Phosphoprotein-protein interactions revealed by the crystal structure of kinase-associated phosphatase in complex with phosphoCDK2. Mol Cell *7*, 615-626.
Tarricone, C., Dhavan, R., Peng, J., Areces, L. B., Tsai, L. H., and Musacchio, A. (2001). Structure and regulation of the CDK5-p25(nck5a) complex. Mol Cell *8*, 657-669.
Taylor, S. S., Knighton, D. R., Zheng, J., Ten Eyck, L. F., and Sowadski, J. M. (1992). Structural framework for the protein kinase family. Annu Rev Cell Biol *8*, 429-462.
Tong, L., Pav, S., White, D. M., Rogers, S., Crane, K. M., Cywin, C. L., Brown, M. L., and Pargellis, C. A. (1997). A highly specific inhibitor of human p38 MAP kinase binds in the ATP pocket. Nat Struct Biol *4*, 311-316.
VanderWel, S. N., Harvey, P. J., McNamara, D. J., Repine, J. T., Keller, P. R., Quin, J., 3rd,

Booth, R. J., Elliott, W. L., Dobrusin, E. M., Fry, D. W., and Toogood, P. L. (2005). Pyrido[2,3-d]pyrimidin-7-ones as specific inhibitors of cyclin-dependent kinase 4. J Med Chem *48*, 2371-2387.

Zhu, L., Harlow, E., and Dynlacht, B. D. (1995). p107 uses a p21CIP1-related domain to bind cyclin/cdk2 and regulate interactions with E2F. Genes Dev *9*, 1740-1752.